
AutoHAS: Differentiable Hyper-parameter and Architecture Search

Xuanyi Dong^{1,2,*}, Mingxing Tan¹, Adams Wei Yu¹, Daiyi Peng¹, Bogdan Gabrys², Quoc V. Le¹
¹Google Research, Brain Team ²AAI, University of Technology Sydney
xuanyi.dxy@gmail.com, {tanmingxing, adamsyuwei, daiyip, qv1}@google.com, bogdan.gabrys@uts.edu.au

Abstract

Neural Architecture Search (NAS) has achieved significant progress in pushing state-of-the-art performance. While previous NAS methods search for different network architectures with the same hyper-parameters, we argue that such search would lead to sub-optimal results. We empirically observe that different architectures tend to favor their own hyper-parameters. In this work, we extend NAS to a broader and more practical space by combining hyper-parameter and architecture search. As architecture choices are often categorical whereas hyper-parameter choices are often continuous, a critical challenge here is how to handle these *two* types of values in a joint search space. To tackle this challenge, we propose *AutoHAS*, a differentiable hyper-parameter and architecture search approach, with the idea of discretizing the continuous space into a linear combination of multiple categorical basis. A key element of AutoHAS is the use of weight sharing across all architectures and hyper-parameters which enables efficient search over the large joint search space. Experimental results on MobileNet/ResNet/EfficientNet/BERT show that AutoHAS significantly improves accuracy up to 2% on ImageNet and F1 score up to 0.4 on SQuAD 1.1, with search cost comparable to training a single model. Compared to other AutoML methods, such as random search or Bayesian methods, AutoHAS can achieve better accuracy with 10x less compute cost.

1 Introduction

Neural Architecture Search (NAS) has brought significant improvements in many applications, such as machine perception [19, 48, 5, 51, 50], language modeling [32, 11], and model compression [17, 10, 16]. Most NAS works apply the *same* hyper-parameters while searching for network architectures. For example, all models in [55, 47, 53] are trained with the same optimizer, learning rate, and weight decay. As a result, the relative ranking of models in the search space is *only* determined by their architectures. However, we observe that different models favor different hyper-parameters. Table 1 shows the performance of two randomly sampled models with different hyper-parameters: under hyper-parameter HP_1 , $model_1$ outperforms $model_2$, but $model_2$ is better under HP_2 . These results suggest using fixed hyper-parameters in NAS would lead to sub-optimal results.

A natural question is: could we extend NAS to a broader scope for joint Hyper-parameter and Architecture Search (HAS)? In HAS, each model can potentially be coupled with its own best hyper-parameters, thus achieving better performance than existing NAS with *fixed* hyper-parameters. However, jointly searching for architectures and hyper-parameters is challenging. The first challenge is how to deal with both categorical and continuous values in the joint HAS search space. While

Table 1: ImageNet accuracy of two models randomly sampled from search space based on MobileNet-V2 [41]. $Model_1$ favors HP_1 while $Model_2$ favors HP_2 .

	$Model_1$	rank	$Model_2$
HP_1 (LR=5.5, L2=1.5e-4)	56.9%	>	55.6%
HP_2 (LR=1.1, L2=8.4e-4)	54.7%	<	56.2%

*This work was done when Xuanyi Dong was a research intern with Google Research, Brain Team.

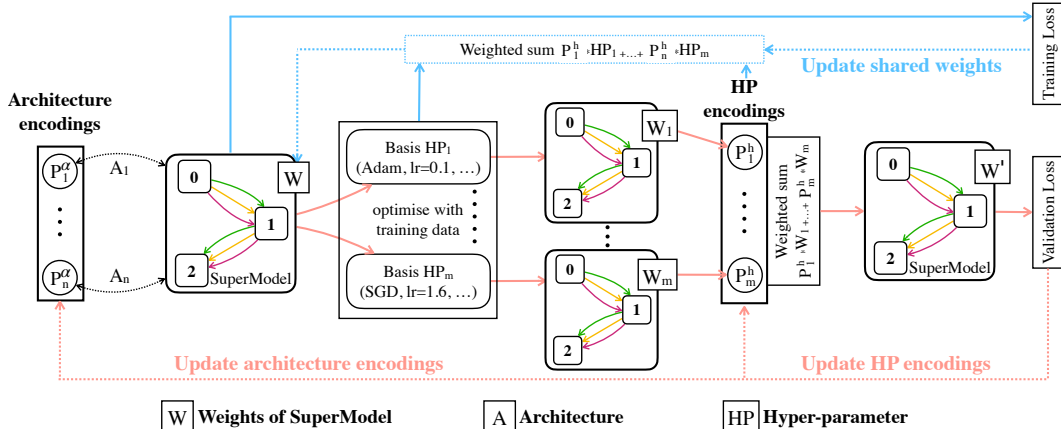


Figure 1: The AutoHAS framework. Architecture encoding $(P_1^\alpha, \dots, P_n^\alpha)$ and hyper-parameter (HP) encoding (P_1^h, \dots, P_m^h) represent the distribution of possible choices. Similar to [38, 32], we use a SuperModel to share the weights among all candidate architectures. AutoHAS alternates between updating the shared weights W and updating the encoding $(P_i^\alpha$ and $P_i^h)$. When updating encoding, each HP basis combination will result in a separate copy of the model weights (W_1, \dots, W_m) . These copies are weighted by the HP encoding to compute the final weights W' . Encoding is updated by back-propagation to minimize validation loss. When updating the shared weights, we first forward the SuperModel to compute the training loss. Then, different HP basis are weighted by the HP encoding to compute one set of hyper-parameters, which will be used to back-propagate the gradients from the training loss to update the shared weights W . After this searching procedure, AutoHAS will derive the final architecture and hyper-parameters from the learned architecture and HP encodings.

architecture choices are mostly categorical values (e.g., convolution kernel size), hyper-parameters choices can be both categorical (e.g., the type of optimizer) and continuous values (e.g., weight decay). There is not yet a good solution to tackle this challenge: previous NAS methods *only* focus on categorical search spaces, while hyper-parameter optimization methods *only* focus on continuous search spaces. They thus cannot be directly applied to such a mixture of categorical and continuous search space. Secondly, another critical challenge is how to efficiently search over the larger joint HAS search space as it combines both architecture and hyper-parameter choices.

In this paper, we propose AutoHAS, a differentiable HAS algorithm. It is, to the best of our knowledge, the first algorithm that can efficiently handle the large joint HAS search space. To address the mixture of categorical and continuous search spaces, we first discretize the continuous hyper-parameters into a linear combination of multiple categorical basis, then we can unify them during search. As explained below, we will use a differentiable method to search over the combination, i.e., architecture and HP encodings in Fig. 1. These encodings represent the probability distribution over all candidates in the respective space. They can be used to find the best architecture together with its associated hyper-parameters.

To efficiently navigate the much larger search space, we further introduce a novel weight sharing technique for AutoHAS. Weight sharing has been widely used in previous NAS approaches [38, 32] to reduce the search cost. The main idea is to train a SuperModel, where each candidate in the architecture space is its sub-model. Using a SuperModel can avoid training millions of candidates from scratch [32, 11, 6, 38]. Motivated by the weight sharing in NAS, AutoHAS extends its scope from architecture search to both architecture and hyper-parameter search. We not only share the weights of the SuperModel with each architecture but also share this SuperModel across hyper-parameters. At each search step, AutoHAS optimizes the shared SuperModel by a combination of the basis of HAS space, and the shared SuperModel serves as a good initialization for all hyper-parameters at the next step of search (see Fig. 1 and Sec. 3).

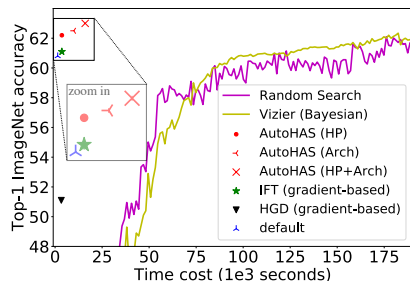


Figure 2: AutoHAS achieves higher accuracy with 10× less search cost than other AutoML methods. We search for the LR, L2, kernel size, expansion of EfficientNet-A0.

In this paper, we focus on architecture, learning rate, and L2 penalty weight optimization, but it should be straightforward to apply AutoHAS to other hyper-parameters. A summary of our results is in Fig. 2, which shows that AutoHAS outperforms many AutoML methods regarding both accuracy and efficiency (more details in Sec. 4.3). In Sec. 4, we show that it improves a number of computer vision and natural language processing models, i.e., MobileNet-V2 [41], ResNet [18], EfficientNet [47], and BERT fine-tuning [8].

2 Related Works

Neural Architecture Search (NAS). Since the seminal works [1, 55] show promising improvements over manually designed architectures, more efforts have been devoted to NAS. The accuracy of the found architectures has been improved by carefully designed search space [56], better search method [40], or compound scaling [47]. The model size and latency of the searched architectures have been reduced by Pareto optimization [46, 50, 6, 5] and enlarged search space of network size [5, 10]. The efficiency of NAS algorithms has been improved by weight sharing [38], differentiable optimization [32], or stochastic sampling [11, 52]. These methods have found state-of-the-art architectures, however, their performance is bounded by the fixed or manually tuned hyper-parameters.

Hyper-parameter optimization (HPO). Black-box and multi-fidelity HPO methods have a long standing history [4, 20, 21, 22, 27, 22]. Black-box methods, e.g., grid search and random search [4], regard the evaluation function as a black-box. They sample some hyper-parameters and evaluate them one by one to find the best. Bayesian methods can make the sampling procedure in random search more efficient [25, 43, 44]. They employ a surrogate model and an acquisition function to decide which candidate to evaluate next [49]. Multi-fidelity optimization methods accelerate the above methods by evaluating on a proxy task, e.g., using less training epochs or a subset of data [9, 23, 27, 31]. These HPO methods are computationally expensive to search for deep learning models [30].

Recently, gradient-based HPO methods have shown better efficiency [2, 33], by computing the gradient with respect to the hyper-parameters. For example, Maclaurin et al. [35] calculate the extract gradients w.r.t. hyper-parameters. Fabian [37] leverages the implicit function theorem to calculate approximate hyper-gradient. Following that, different approximation methods have been proposed [33, 37, 42]. Despite of their efficiency, they can only be applied to differentiable hyper-parameters such as weight decay, but not non-differentiable hyper-parameters, such as learning rate [33] or optimizer [42]. Our AutoHAS is not only as efficient as gradient-based HPO methods but also applicable to both differentiable and non-differentiable hyper-parameters. Moreover, we show significant improvements on state-of-the-art models with large-scale datasets, which supplements the lack of strong empirical evidence in previous HPO methods.

Joint Hyper-parameter and Architecture Search (HAS). Few approaches have been developed for the joint searching of HAS [26, 54]. However, they focus on small datasets and small search spaces. These methods are more computationally expensive than our AutoHAS.

3 AutoHAS

3.1 Preliminaries

HAS aims to find architecture α and hyper-parameters h that achieve high performance on the validation set. HAS can be formulated as a bi-level optimization problem:

$$\min_{\alpha, h} \mathcal{L}(\alpha, h, \omega_{\alpha}^*, \mathbb{D}_{val}) \quad \text{s.t.} \quad \omega_{\alpha}^* = f_h(\alpha, \omega_{\alpha}^0, \mathbb{D}_{train}), \quad (1)$$

where \mathcal{L} indicates the objective function (e.g., cross-entropy loss) and ω_{α}^0 indicates the initial weights of the architecture α . \mathbb{D}_{train} and \mathbb{D}_{val} denote the training data and the validation data, respectively. f_h represents the algorithm with hyper-parameters h to obtain the optimal weights ω_{α}^* , such as using SGD to minimize the training loss. In that case, $\omega_{\alpha}^* = f_h(\alpha, \omega_{\alpha}^0, \mathbb{D}_{train}) = \arg \min_{\omega_{\alpha}} \mathcal{L}(\alpha, h, \omega_{\alpha}^0, \mathbb{D}_{train})$. We can also use HyperNetwork [15] to generate weights ω_{α}^* .

HAS generalizes both NAS and HPO by introducing a broader search space. On one-hand, NAS is a special case of HAS, where the inner optimization $f_h(\alpha, \omega_{\alpha}^0, \mathbb{D}_{train})$ uses fixed α and h to optimize $\min_{\omega} \mathcal{L}(\alpha, h, \omega, \mathbb{D}_{train})$. On the other, HPO is a special case of HAS, where α is fixed in Eq. (1).

3.2 Representation of the HAS Search Space in AutoHAS

The search space of HAS in AutoHAS is a Cartesian product of the architecture and hyper-parameter candidates. To search over this mixed search space, we need a unified representation of different searchable components, i.e., architectures, learning rates, optimizers, etc.

Architectures Search Space. We use the simplest case as an example. First of all, let the set of predefined candidate operations (e.g., 3x3 convolution, pooling, etc.) be $\mathcal{O} = \{O_1, O_2, \dots, O_n\}$, where the cardinality of \mathcal{O} is n . Suppose an architecture is constructed by stacking multiple layers, each layer takes a tensor F as input and output $\pi(F)$, which serves as the next layer’s input. $\pi \in \mathcal{O}$ denotes the operation at a layer and might be different at different layers. Then a candidate architecture α is essentially the sequence for all layers $\{\pi\}$. Further, a layer can be represented as a linear combination of the operations in \mathcal{O} as follows:

$$\pi(F) = \sum_{i=1}^n P_i^\alpha O_i(F) \quad \text{s.t. } P_i^\alpha \in \{0, 1\}, \sum_{i=1}^n P_i^\alpha = 1, \quad (2)$$

where P_i^α (the i -th element of the vector P^α) is the coefficient of operation O_i for a layer. We call the set of all coefficients $\mathcal{A} = \{P^\alpha \text{ for all layers}\}$ the *architecture encoding*, which can then represent the search space of the architecture.

Hyper-parameter Search Space. Now we can define the hyper-parameter search space in a similar way. The major difference is that we have to consider both categorical and continuous cases:

$$h = \sum_{i=1}^m P_i^h \mathcal{B}_i \quad \text{s.t. } \sum_{i=1}^m P_i^h = 1, P_i^h \in \begin{cases} [0, 1], & \text{if continuous} \\ \{0, 1\}, & \text{if categorical} \end{cases} \quad (3)$$

where \mathcal{B} is a predefined set of hyper-parameter basis with the cardinality of m and \mathcal{B}_i is the i -th basis in \mathcal{B} . P_i^h (the i -th element of the vector P^h) is the coefficient of hyper-parameter basis \mathcal{B}_i . If we have a continuous hyper-parameter, we have to discretize it into a linear combination of basis and unify both categorical and continuous. For example, for weight decay, \mathcal{B} could be $\{1e-1, 1e-2, 1e-3\}$, and therefore, all possible weight decay values can be represented as a linear combination over \mathcal{B} . For categorical hyper-parameters, taking the optimizer as an example, \mathcal{B} could be $\{\text{Adam, SGD, RMSProp}\}$. In this case, a constraint on P_i^h is applied: $P_i^h \in \{0, 1\}$ as in Eq. (3). When there are multiple different types of hyper-parameters, each of them will have their own P^h . The hyper-parameter basis becomes the Cartesian product of their own basis and the coefficient is the product of the corresponding P_i^h . We name the set of all coefficients $\mathcal{H} = \{P^h \text{ for all types of hyper-parameter}\}$ the *hyper-parameter encoding*, which can then represent the search space of hyper-parameters.

3.3 AutoHAS: Automated Hyper-parameter and Architecture Search

Since each candidate in the HAS search space can be represented by a pair of \mathcal{H} and \mathcal{A} , the searching problem is converted to optimizing the encoding \mathcal{H} and \mathcal{A} . However, it is computationally prohibitive to compute the exact gradient of $\mathcal{L}(\alpha, h, \omega_\alpha^*, \mathbb{D}_{val})$ in Eq. (1) w.r.t. \mathcal{H} and \mathcal{A} . Alternatively, we propose a simple approximation strategy with weight sharing to accelerate this procedure.

First of all, we leverage a SuperModel to share weights among all candidate architectures in the architecture space, where each candidate is a sub-model in this SuperModel [38, 32]. The weights of the SuperModel \mathcal{W} is the union of weights of all basis operations in each layer. The weights ω_α of an architecture α can thus be represented by \mathcal{W}_α , a subset of \mathcal{W} . Computing the exact gradients of \mathcal{L} w.r.t. \mathcal{H} and \mathcal{A} requires back-propagating through the initial network state \mathcal{W}_α^0 , which is too expensive. Inspired by [32, 38], we approximate it using the current SuperModel weight \mathcal{W} as follows:

$$\nabla_{\mathcal{A}, \mathcal{H}} \mathcal{L}(\alpha, h, \omega_\alpha^*, \mathbb{D}_{val}) \approx \nabla_{\mathcal{A}, \mathcal{H}} \mathcal{L}(\alpha, h, f_h(\alpha, \mathcal{W}_\alpha, \mathbb{D}_{train}), \mathbb{D}_{val}), \quad (4)$$

Ideally, we should back-propagate \mathcal{L} through f_h to modify the encoding \mathcal{H} . However, f_h might be a complex optimization algorithm and not allow back-propagation. To solve this problem, we regard f as a black-box function and reformulate f_h as follows:

$$f_h(\alpha, \mathcal{W}_\alpha, \mathbb{D}_{train}) \approx \sum_{i=1}^m P_i^h f_{\mathcal{B}_i}(\alpha, \mathcal{W}_\alpha, \mathbb{D}_{train}), \quad (5)$$

In this way, $f_h(\alpha, \mathcal{W}_\alpha, \mathbb{D}_{train})$ is calculated as a weighted sum of P_i^h and generated weights from $f_{\mathcal{B}_i}$.

In practice, it is not easy to directly optimize the encodings \mathcal{A} and \mathcal{H} , because they naturally have some constraints associated with them, such as Eq. (3). Inspired by the continuous relaxation [32, 11], we instead use another set of relaxed variables $\tilde{\mathcal{A}} = \{\tilde{P}^\alpha \text{ for all layers}\}$ and

$\tilde{\mathcal{H}} = \{\tilde{P}^h \text{ for all types of hyper-parameters}\}$ to calculate \mathcal{A} and \mathcal{H} . \tilde{P}^α and \tilde{P}^h have the same dimension as P^α and P^h . The calculation procedure encapsulates the constraints of P^α and P^h in Eq. (2) and Eq. (3) as follows:

$$P^h = \text{one_hot}(\arg \max_j \tilde{P}_j^h), \quad (6)$$

$$\tilde{P}_i^h = \frac{\exp((\hat{P}_i^h + \mathbf{o}_i)/\tau)}{\sum_k \exp((\hat{P}_k^h + \mathbf{o}_k)/\tau)}, \quad \text{where} \quad \hat{P}_i^h = \frac{\exp(\tilde{P}_i^h)}{\sum_k \exp(\tilde{P}_k^h)}, \quad (7)$$

$$\mathbf{o}_k = -\log(-\log(u)), \quad \text{where} \quad u \sim \text{Uniform}[0, 1], \quad (8)$$

where P^h is computed by applying the Gumbel-Softmax function [24, 36] on \tilde{P}^h . τ is a temperature value and \mathbf{o}_k are i.i.d samples drawn from Gumbel (0,1). The Gumbel-Softmax in Eq. (7) incorporates the stochastic procedure during search. It can help explore more candidates in the HAS search space and avoid over-fitting to some sub-optimal architecture and hyper-parameters. We use the same procedure as Eq. (6)~(8) to define \tilde{P}^α and \hat{P}^α for architecture encodings. Ideally, the encodings should be optimized with Eq. (6) by back-propagation, but unfortunately one-hot encodings P^h and P^α are not differentiable. To address this issue, we follow [11, 24, 36] to relax the one-hot encodings: in the forward pass, we use one-hot encodings P^h to compute validation loss, but in the backward pass, we apply relaxation on P^h and substitute $\frac{\partial P^h}{\partial P^h}$ by $\frac{\partial \tilde{P}^h}{\partial \tilde{P}^h}$ during back-propagation.

We describe our AutoHAS algorithm in Algorithm 1. During search, we jointly optimize \mathcal{W} and $(\tilde{\mathcal{A}}, \tilde{\mathcal{H}})$ in an iterative way. The \mathcal{W} is updated as follows:

$$\mathcal{W}_\alpha \leftarrow f_h(\alpha, \mathcal{W}_\alpha, \mathbb{D}_{train}), \quad (9)$$

where f_h is a training algorithm: in our experiments, it is implemented as minimizing the training loss with respect to hyper-parameter h by one step. Notably, in Eq. (9), h is computed by $\tilde{\mathcal{H}}$ and α is computed by $\tilde{\mathcal{A}}$.

3.4 Deriving Hyper-parameters and Architecture

After obtaining the optimized encoding of architecture $\tilde{\mathcal{A}} = \{\tilde{P}^\alpha\}$ and hyper-parameters $\tilde{\mathcal{H}} = \{\tilde{P}^h\}$ following Sec. 3.3, we use them to derive the final architecture and hyper-parameters. For hyper-parameters, we apply different strategies to the continuous and categorical values:

$$P^h = \begin{cases} \hat{P}^h & \text{if continuous} \\ \text{one_hot}(\arg \max_i \hat{P}_i^h) & \text{if categorical} \end{cases}, \quad (10)$$

For architectures, since all values are categorical, we apply the same strategy in Eq. (10) for categorical values.

Notably, unlike other fixed hyper-parameters, the learning rate can have different values at each training step, so it is a list of continuous values instead of a single scalar. To deal with this special case, we use Eq. (10) to derive the continuous learning rate value at each searching step, such that we can obtain a list of learning rate values corresponding to each specific step.

After we derive the final architecture and hyper-parameters as in Algorithm 1, we will use the searched hyper-parameters to re-train the searched architecture.

4 Experiments

4.1 Experimental Settings

Datasets. We demonstrate the effectiveness of our AutoHAS on five vision datasets, i.e., ImageNet [7], Birdsnap [3], CIFAR-10, CIFAR-100 [29], and Cars [28], and a NLP dataset, i.e., SQuAD 1.1 [39].

Searching settings. We call the hyper-parameters that control the behavior of AutoHAS as meta hyper-parameters. For the meta hyper-parameters, we set $\tau = 10$ in Gumbel-Softmax and employ Adam optimizer with a fixed learning rate 0.002. Notably, we use the same meta hyper-parameters for all search experiments. The number of searching epochs and batch size are set to be the same as in

Algorithm 1 The AutoHAS Procedure

Input: Randomly initialize \mathcal{W}

Input: Randomly initialize $(\tilde{\mathcal{A}}, \tilde{\mathcal{H}})$

Input: Split the available data into two disjoint sets: \mathbb{D}_{train} and \mathbb{D}_{val}

1: **while** not converged **do**

2: Update weights \mathcal{W} via Eq. (9)

3: Optimize $(\tilde{\mathcal{A}}, \tilde{\mathcal{H}})$ via Eq. (4)~(8)

4: **end while**

5: Derive the final architecture from $\tilde{\mathcal{A}}$ and hyper-parameters from $\tilde{\mathcal{H}}$

the training settings of baseline models, i.e., they can be different for different baseline models. When searching for MBConv-based models [46, 41], we search for the kernel size from {3, 5, 7} and the expansion ratio from {3, 6}. For vision tasks, the hyper-parameter basis for the continuous value is the product of the default value and multipliers {0.1, 0.25, 0.5, 0.75, 1.0, 2.5, 5.0, 7.5, 10.0}. For the NLP task, we use smaller multipliers {0.01, 0.05, 0.1, 0.5, 1.0, 1.2, 1.5} since they are for fine-tuning on top of pretrained models. If a model has a default learning rate schedule, we create a range of values around the default learning rate at each step and use AutoHAS to find the best learning rate at each step.

Training settings. On vision datasets, we use six models, i.e., three variants of MobileNet-V2 (MNet2), EfficientNet-A0 (ENet-A0), ResNet-18, and ResNet-50. We use the batch size of 4096 for ImageNet and 1024 for other vision datasets. We use the same data augmentation as shown in [18]. On the NLP dataset SQuAD, we fine-tune the pretrained BERT_{LARGE} model and follow the setting of [8]. The number of training epochs is different for different datasets, and we will explain their details later. For learning rate and weight decay, we use the values found by AutoHAS.

4.2 Ablation Studies

We did a series of experiments to study the effect of (I) different searching strategies; (II) different deriving strategies; (III) AutoHAS-searched vs. manually tuned hyper-parameters.

The effect of searching strategies. One of the key questions in searching is how to relax and optimize the architecture and hyper-parameter encodings. Our AutoHAS leverages Gumbel-Softmax in Eq. (7) to stochastically explore different hyper-parameter and architecture basis. We evaluate two different variants in Table 2. “Softmax” does not add the Gumbel distributed noise and performs poorly compared to using Gumbel-Softmax. This strategy has an over-fitting problem, which is also found in NAS [11, 52, 12, 50]. “GS (soft)” does not use the one-hot vector in Eq. (7) and thus it will explore too many hyper-parameters during searching. As a result, its optimization might become difficult and the found are worse than AutoHAS.

The effect of deriving strategies. We evaluate two kinds of strategies to derive the final hyper-parameters and architectures. The vanilla strategy is to follow previous NAS methods: selecting the basis hyper-parameters with the maximal probability. However, it does not work well for the continuous choices. As shown in Table 2, our proposed strategy “GS (hard) + Eq. (10)” can improve the accuracy by 1.1% compared to the vanilla strategy “GS (hard) + Eq. (6)”.

Searched hyper-parameters vs. manually tuned hyper-parameters. We show the searched and manually tuned hyper-parameters in Fig. 3. For the weight of L2 penalty, it is interesting that AutoHAS indicates using large penalty for the large models (ResNet) at the beginning and decay it to a smaller value at the end of searching. For manual tuning, you need to tune every model one by one to obtain their optimal hyper-parameters. In contrast, AutoHAS only requires to tune *two* meta hyper-parameters, in which it can successfully find good hyper-parameters for tens of models. Besides,

Table 2: We analyze different strategies used in AutoHAS. “GS” indicates Gumbel-Softmax. “hard” indicates using one-hot in forward pass and relaxation during backward pass. “soft” indicates using relaxation during both forward and backward passes.

Searching Strategy	Deriving Strategy	MNet2 (S0)	MNet
Softmax	Eq. (6)	44.0%	63.5%
GS (soft)	Eq. (6)	45.5%	65.2%
GS (hard)	Eq. (6)	45.9%	66.4%
Softmax	Eq. (10)	40.8%	61.4%
GS (soft)	Eq. (10)	41.5%	67.0%
GS (hard)	Eq. (10)	46.3%	67.5%

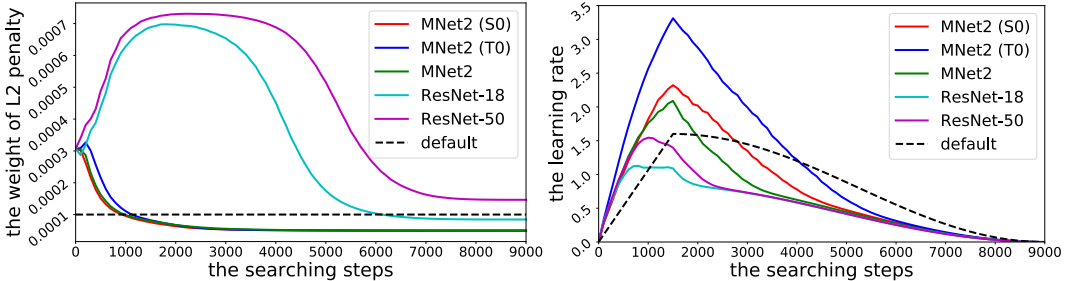


Figure 3: AutoHAS found different learning rate and weight of L2 penalty for different models.

Table 3: We compare four AutoML algorithms [4, 13, 2, 33] on four search spaces. “-” indicates the algorithm can not be applied to that search space. We choose the hyper-parameters in ResNet [18] with warm-up mechanism [34] as the default setting (“default HP”) to train models on ImageNet. The number of training epochs is 30. “RS” indicates the random searching algorithm [4]. “N/A” indicates the corresponding searching algorithm can not be applied. “ENet” and “MNet2” indicate EfficientNet and MobileNet-V2, respectively. “A+LR+L2” indicates searching for architecture, learning rate, and weight of L2 penalty. For AutoHAS, we use the *same meta hyper-parameters* for all searching experiments: Adam with the learning rate of 0.002, τ of 10, and the same multipliers to create basis.

Type	Model	Searching Methods					
		default HP	RS [4]	Vizier [13]	IFT [33]	HGD [2]	AutoHAS
LR	MNet2 (S0)	44.6±0.6	12.3±8.7	6.1±4.5	N/A	29.6±2.1	44.8±0.4
	MNet2 (T0)	52.4±0.5	17.5±3.0	14.3±20.0	N/A	33.0±4.4	52.0±0.2
	MNet2	66.8±0.2	38.9±5.6	49.0±3.6	N/A	49.1±4.6	66.9±0.1
	ENet-A0	60.8±0.0	46.6±1.2	50.8±0.8	N/A	50.0±1.4	61.0±0.0
	ResNet-18	67.6±0.1	60.4±1.2	63.5±0.2	N/A	56.3±0.5	67.9±0.2
	ResNet-50	74.8±0.1	67.2±0.1	71.1±0.3	N/A	62.3±0.3	75.2±0.1
L2	MNet2 (S0)	44.6±0.6	45.9±0.7	46.3±0.2	46.2±0.1	N/A	46.3±0.1
	MNet2 (T0)	52.4±0.5	52.2±0.0	52.4±0.4	52.5±0.2	N/A	53.5±0.3
	MNet2	66.8±0.2	66.4±0.8	67.0±0.2	66.4±0.2	N/A	67.5±0.1
	ENet-A0	60.8±0.0	60.0±2.0	62.0±0.2	61.1±0.2	N/A	62.2±0.1
	ResNet-18	67.6±0.1	67.9±0.2	67.6±0.1	66.6±0.3	N/A	67.9±0.0
	ResNet-50	74.8±0.1	75.0±0.1	74.8±0.1	73.1±0.4	N/A	75.0±0.1
LR +L2	MNet2 (S0)	44.6±0.6	13.1±10.9	15.2±7.3	N/A	N/A	45.7±0.3
	MNet2 (T0)	52.4±0.5	29.3±20.6	30.2±15.9	N/A	N/A	53.8±0.2
	MNet2	66.8±0.2	21.6±15.1	25.2±14.6	N/A	N/A	67.3±0.1
	ENet-A0	60.8±0.0	47.3±4.7	49.3±2.4	N/A	N/A	61.5±0.1
	ResNet-18	67.6±0.1	54.2±8.5	53.5±0.5	N/A	N/A	67.8±0.0
	ResNet-50	74.8±0.1	67.4±4.7	66.7±1.9	N/A	N/A	74.8±0.1
A+LR +L2	MNet2 (S0)	44.6±0.6	22.4±12.4	25.4±4.1	46.4±0.4	N/A	47.5±0.3
	ENet-A0	60.8±0.0	53.4±5.7	56.4±3.9	61.8±0.5	N/A	62.9±0.2

Table 4: We report the computational costs of each model and the searching costs of each AutoML algorithm on ImageNet. Since the time may vary on batch size, platforms, accelerators, or devices, we also report the relative cost to the training time. We use the same notation as used in Table 3.

Model	Params (MB)	FLOPs (M)	Train Time (seconds)	Searching Methods			
				RS / Vizier	IFT-Neumann	HGD	AutoHAS
MNet2 (S0)	1.49	35.0	2.0e3	1.9e4 (9.4×)	2.0e3 (1.0×)	2.6e3 (1.3×)	2.8e3 (1.4×)
MNet2 (T0)	1.77	89.5	2.1e3	2.0e4 (9.3×)	2.5e3 (1.2×)	4.1e3 (2.0×)	2.4e3 (1.2×)
MNet2	3.51	307.3	2.4e3	1.8e4 (7.5×)	5.7e3 (2.3×)	2.5e3 (1.1×)	4.7e3 (1.9×)
ENet-A0	2.17	76.2	1.4e3	1.2e4 (8.7×)	2.2e3 (1.6×)	1.9e3 (1.4×)	2.2e3 (1.6×)
ResNet-18	11.69	1818	2.0e3	1.9e4 (9.6×)	2.7e3 (1.4×)	2.2e3 (1.1×)	2.2e3 (1.1×)
ResNet-50	25.56	4104	2.6e3	2.0e4 (7.6×)	2.9e3 (1.1×)	2.8e3 (1.1×)	2.8e3 (1.1×)

some hyper-parameters, such as learning rate, are dynamically changed for every training step. It is hard for human to tune its per-step value, while AutoHAS can deal with such hyper-parameters.

4.3 AutoHAS for Vision Datasets

ImageNet: We first apply AutoHAS to ImageNet and compare the performance with previous AutoML algorithms. We choose the hyper-parameters used for ResNet [18] as our default hyper-parameters: warm-up the learning rate at the first 5 epochs from 0 to $0.1 \times \frac{\text{batch size}}{256}$ and decay it to 0 via cosine annealing schedule [14]; use the weight of L2 penalty as 1e-4. Since these hyper-parameters have been heavily tuned by human experts, there is limited headroom to improve. Therefore, we study how to train a model to achieve a good performance in shorter time, i.e., 30 epochs.

Table 3 and Table 4 shows the performance comparison. There are some interesting observations: (I) AutoHAS is applicable to searching for almost all kinds of hyper-parameters and architectures, while

previous hyper-gradient based methods [33, 2] can only be applied to some hyper-parameters. (II) AutoHAS shows improvements in seven different representative models, including both light-weight and heavy models. (III) The found hyper-parameters by AutoHAS outperform the (default) manually tuned hyper-parameters. (IV) The found hyper-parameters by AutoHAS outperform that found by other AutoML algorithms. (V) Searching over the large joint HAS search space can obtain better results compared to searching for hyper-parameters only. (VI) Gradient-based AutoML algorithms are more efficient than black-box optimization methods, such as random search and vizier.

Smaller datastes: To analyze the effect of architecture and hyper-parameters, we compare AutoHAS with two variants: searching for architecture only, i.e., GDAS (Arch), and searching for hyper-parameters only, i.e., AutoHAS (HP). The results on four datasets are shown in Table 5. On Birdsnap and Cars, AutoHAS significantly outperforms GDAS (Arch) and AutoHAS (HP). On CIFAR-100, the accuracy of AutoHAS is similar to GDAS (Arch) and AutoHAS (HP), while all of them outperform the default. On CIFAR-10, the accuracy of auto-tuned architecture or hyper-parameters is similar or slightly lower than the default. It might because the default choices are close to the optimal solution in the current HAS search space on CIFAR-10.

Table 5: We use AutoHAS to search for hyper-parameters (HP), architectures (Arch), and both hyper-parameters and architectures (HP+Arch) on four datasets. We use MobileNet-V2 as the default model. We follow Table 3 to setup the default hyper-parameters. For all datasets, AutoHAS either outperforms or is competitive to searching HP or Arch only.

	Birdsnap	CIFAR-10	CIFAR-100	Cars
default	51.7±0.7	93.9±0.2	75.7±0.2	72.0±0.8
GDAS (Arch) [11]	55.8±0.6	93.5±0.0	76.4±0.5	77.0±2.5
AutoHAS (HP)	54.4±0.7	93.9±0.1	76.0±0.1	77.7±0.1
AutoHAS (HP+Arch)	56.5±0.9	93.7±0.3	76.0±0.4	80.3±0.5

4.4 AutoHAS for SQuAD

To further validate the generalizability of AutoHAS, we also conduct experiments on a reading comprehension dataset in the NLP domain, i.e., SQuAD 1.1 [39]. We pretrain a BERT_{LARGE} model following [8] and then apply AutoHAS when fine-tuning it on SQuAD 1.1. In particular, we search the per-step learning rate and weight decay of Adam. For AutoHAS, we split the training set of SQuAD 1.1 into 80% for training and 20% validation. In Fig. 4, we show the results on the dev set, and compare the default setup in [8] with hyper-parameters found by AutoHAS. We vary the fine-tuning steps from 2K to 22K and each setting is run 5 times. We can see that AutoHAS is superior to the default hyper-parameters under most of the circumstances, in terms of both F1 and exact match (EM) scores. Notably, the average gain on F1 over all the steps is 0.3, which is highly nontrivial.²

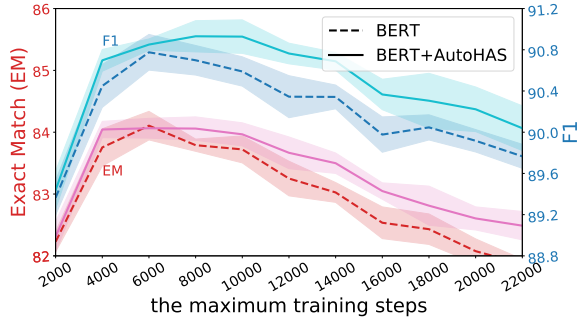


Figure 4: Performance comparison on SQuAD 1.1 fine-tuned on the BERT_{LARGE} model. AutoHAS achieves better performance in both F1 and exact match (EM) than the default setting in [8] under various maximum training steps over 5 runs.

5 Conclusion

In this paper, we study the joint search of hyper-parameters and architectures. Our framework overcomes the unrealistic assumptions in NAS that the relative ranking of models’ performance is primarily affected by their architecture. To address the challenge of joint search, we proposed AutoHAS, i.e., an efficient and differentiable searching algorithm for both hyper-parameters and architecture. AutoHAS represents the hyper-parameters and architectures in a unified way to handle the mixture of categorical and continuous values of the search space. AutoHAS shares weights across all hyper-parameters and architectures, which enable it to search efficiently over the joint large search space. Experiments on both large-scale vision and NLP datasets demonstrate the effectiveness of AutoHAS.

²As of 06/03/2020, it takes 11-months effort for the best model LUKE of SQuAD 1.1 to outperform the runner-up XLNet on F1 by 0.3 (see <https://rajpurkar.github.io/SQuAD-explorer/>).

A More Experimental Details

A.1 Datasets

We use five vision datasets and a NLP dataset to validate the effectiveness of our AutoHAS.

The ImageNet dataset [7] is a large scale image classification dataset, which has 1.28 million training images and 50 thousand images for validation. All images in ImageNet are categorized into 1000 classes. During searching, we split the training images into 1231121 images to optimize the weights and 50046 images to optimize the encoding.

The Birdsnap dataset [3] is for fine-grained visual classification, with 49829 images for 500 species. There are 47386 training images and 2443 test images. During searching, we split the training images into 42405 images to optimize the weights and 4981 images to optimize the encoding.

The CIFAR-10 dataset [29] consists of 60000 colour images in 10 classes, with 6000 images per class. There are 50000 training images and 10000 test images. During searching, we split the training images into 45000 images to optimize the weights and 5000 images to optimize the encoding.

The CIFAR-100 dataset [29] is similar to CIFAR-10, while it classifies each image into 100 fine-grained classes. During searching, we split the training images into 45000 images to optimize the weights and 5000 images to optimize the encoding.

The Cars dataset [28] contains 16185 images of 196 classes of cars. The data is split into 8144 training images and 8041 testing images. During searching, we split the training images into 6494 images to optimize the weights and 1650 images to optimize the encoding.

The SQuAD 1.1 dataset [39] is a reading comprehension dataset of 107.7K data examples, with 87.5K for training, 10.1K for validation, and another 10.1K (hidden on server) for testing. Each example is a question-paragraph pair, where the question is generated by crowd-sourced workers, and the answer must be a span from the paragraph, which is also labeled by the worker. In this paper, we train on the training set, and only report the results on validation set. During search, we use 80% of the training data to optimize the weights and the remaining to optimize the encoding.

A.2 Experimental Settings

Hyper-parameters in Table 1. Both HP_1 and HP_2 train the model by 30 epochs in total, warm-up the learning rate from 0 to the peak value in 5 epochs, and then decay the learning rate to 0 by the cosine schedule. The model is trained by momentum SGD. For HP_1 , we use the peak value as 5.5945 and the weight for L2 penalty as 0.000153. For HP_2 , we use the peak value as 1.1634 and the weight for L2 penalty as 0.0008436. Both $Model_1$ and $Model_2$ are similar to MobileNet-V2 but use different kernel size and expansion ratio for the MBConv block. The (kernel size, expansion ratio) in all blocks for Model-1 are $\{(7,1), (3,6), (3,6), (7,3), (3,3), (5,6), (3,6), (7,6), (3,3), (5,3), (5,6), (7,6), (3,6), (3,6), (3,6), (7,3), (3,3)\}$. The (kernel size, expansion ratio) in all blocks for Model-2 are $\{(7,1), (7,3), (5,3), (5,3), (7,6), (5,6), (7,3), (5,6), (3,3), (3,3), (7,6), (3,6), (5,6), (7,6), (7,3), (7,6), (5,6)\}$.

More details in Figure 2. The baseline model is EfficientNet-A0. For Random Search and Vizier, we report their results when searching for both learning rate and the weight of L2 penalty. When searching for the architecture, we search for the kernel size from $\{3, 5, 7\}$ and the expansion ratio from $\{3, 6\}$.

Architecture of six models on ImageNet. We use the standard MobileNet-V2, ResNet-18, and ResNet-50. MNet2 (S0) is similar to MobileNet-V2 but sets the width multiplier and depth multiplier as 0.3. MNet2 (T0) sets the width multiplier as 0.2 and the multiplier as 3.0, thus it is a very thin network. EfficientNet-A0 (ENet-A0) uses the coefficients for scaling network width, depth, and resolution as 0.7, 0.5, and 0.7, respectively.

Data augmentation. On ImageNet, we use the standard data augmentation following [18]. Since we use a large batch size, i.e., 4096, the learning rate is increased to 1.6. By default, we train the model on ImageNet by 30 epochs. On other smaller vision datasets, we apply the same data augmentation as [45], while we resize the image into 112 instead of 224 in ImageNet. We use a relatively small batch size 1024 and the learning rate of 0.4. By default, we train the model on small vision datasets by 9000 iterations.

Architecture and hyper-parameters of BERT. We start with the pre-trained BERT_{LARGE} model [8], whose backbone is essentially a transformer model with 24 layers, 1024 hidden units and 16 heads. When fine-tuning the model on SQuAD 1.1, we adopt the hyper-parameters in [8] as the default values: learning rate warm-up from 0 to 5e-5 for the first 10% training steps and then linearly decay to 0, with a batch size of 32.

Hardware. ImageNet experiments are performed on a 32-core TPUv3, and others are performed on a 8-core TPUv3 by default. When the memory is not enough, we increase the number of cores to meet the memory requirements.

All codes are implemented in Tensorflow. We run each searching experiment three times for the vision tasks and report the mean±variance. For the NLP task, since it is more sensitive than vision task, we run each searching experiment five times and report the mean±variance.

References

- [1] B. Baker, O. Gupta, N. Naik, and R. Raskar. Designing neural network architectures using reinforcement learning. In *International Conference on Learning Representations (ICLR)*, 2017.
- [2] A. G. Baydin, R. Cornish, D. M. Rubio, M. Schmidt, and F. Wood. Online learning rate adaptation with hypergradient descent. In *International Conference on Learning Representations (ICLR)*, 2018.
- [3] T. Berg, J. Liu, S. Woo Lee, M. L. Alexander, D. W. Jacobs, and P. N. Belhumeur. Birdsnap: Large-scale fine-grained visual categorization of birds. In *Proceedings of the IEEE Conference on Computer Vision and Pattern Recognition (CVPR)*, pages 2011–2018, 2014.
- [4] J. Bergstra and Y. Bengio. Random search for hyper-parameter optimization. *The Journal of Machine Learning Research (JMLR)*, 13(Feb):281–305, 2012.
- [5] H. Cai, C. Gan, and S. Han. Once for all: Train one network and specialize it for efficient deployment. In *International Conference on Learning Representations (ICLR)*, 2020.
- [6] H. Cai, L. Zhu, and S. Han. ProxylessNAS: Direct neural architecture search on target task and hardware. In *International Conference on Learning Representations (ICLR)*, 2019.
- [7] J. Deng, W. Dong, R. Socher, L.-J. Li, K. Li, and L. Fei-Fei. ImageNet: A large-scale hierarchical image database. In *Proceedings of the IEEE Conference on Computer Vision and Pattern Recognition (CVPR)*, pages 248–255, 2009.
- [8] J. Devlin, M.-W. Chang, K. Lee, and K. Toutanova. BERT: Pre-training of deep bidirectional transformers for language understanding. In *The Conference of the Association for Computational Linguistics (ACL)*, pages 4171–4186, 2019.
- [9] T. Domhan, J. T. Springenberg, and F. Hutter. Speeding up automatic hyperparameter optimization of deep neural networks by extrapolation of learning curves. In *International Joint Conference on Artificial Intelligence (IJCAI)*, pages 3460–3468, 2015.
- [10] X. Dong and Y. Yang. Network pruning via transformable architecture search. In *The Conference on Neural Information Processing Systems (NeurIPS)*, pages 760–771, 2019.
- [11] X. Dong and Y. Yang. Searching for a robust neural architecture in four gpu hours. In *Proceedings of the IEEE Conference on Computer Vision and Pattern Recognition (CVPR)*, pages 1761–1770, 2019.
- [12] X. Dong and Y. Yang. Nas-bench-201: Extending the scope of reproducible neural architecture search. In *International Conference on Learning Representations (ICLR)*, 2020.
- [13] D. Golovin, B. Solnik, S. Moitra, G. Kochanski, J. Karro, and D. Sculley. Google vizier: A service for black-box optimization. In *The SIGKDD International Conference on Knowledge Discovery and Data Mining*, 2017.
- [14] P. Goyal, P. Dollár, R. Girshick, P. Noordhuis, L. Wesolowski, A. Kyrola, A. Tulloch, Y. Jia, and K. He. Accurate, large minibatch sgd: Training imagenet in 1 hour. *arXiv preprint arXiv:1706.02677*, 2017.
- [15] D. Ha, A. Dai, and Q. V. Le. HyperNetworks. In *International Conference on Learning Representations (ICLR)*, 2017.
- [16] S. Han, H. Mao, and W. J. Dally. Deep compression: Compressing deep neural networks with pruning, trained quantization and huffman coding. In *International Conference on Learning Representations (ICLR)*, 2016.
- [17] J. L. Z. L. H. W. L.-J. L. He, Yihui and S. Han. AMC: Automl for model compression and acceleration on mobile devices. In *Proceedings of the European Conference on Computer Vision (ECCV)*, pages 183–202, 2018.

- [18] K. He, X. Zhang, S. Ren, and J. Sun. Deep residual learning for image recognition. In *Proceedings of the IEEE Conference on Computer Vision and Pattern Recognition (CVPR)*, pages 770–778, 2016.
- [19] A. Howard, M. Sandler, G. Chu, L.-C. Chen, B. Chen, M. Tan, W. Wang, Y. Zhu, R. Pang, V. Vasudevan, et al. Searching for mobilenetv3. In *Proceedings of the IEEE International Conference on Computer Vision (ICCV)*, pages 1314–1324, 2019.
- [20] F. Hutter. *Automated configuration of algorithms for solving hard computational problems*. PhD thesis, University of British Columbia, 2009.
- [21] F. Hutter, H. H. Hoos, and K. Leyton-Brown. Sequential model-based optimization for general algorithm configuration. In *International Conference on Learning and Intelligent Optimization*, pages 507–523, 2011.
- [22] F. Hutter, L. Kotthoff, and J. Vanschoren. *Automated Machine Learning*. Springer, 2019.
- [23] M. Jaderberg, V. Dalibard, S. Osindero, W. M. Czarnecki, J. Donahue, A. Razavi, O. Vinyals, T. Green, I. Dunning, K. Simonyan, et al. Population based training of neural networks. *arXiv preprint arXiv:1711.09846*, 2017.
- [24] E. Jang, S. Gu, and B. Poole. Categorical reparameterization with gumbel-softmax. In *International Conference on Learning Representations (ICLR)*, 2017.
- [25] D. R. Jones, M. Schonlau, and W. J. Welch. Efficient global optimization of expensive black-box functions. *Journal of Global Optimization*, 13(4):455–492, 1998.
- [26] A. Klein and F. Hutter. Tabular benchmarks for joint architecture and hyperparameter optimization. *arXiv preprint arXiv:1905.04970*, 2019.
- [27] R. Kohavi and G. H. John. Automatic parameter selection by minimizing estimated error. In *Machine Learning Proceedings*, pages 304–312, 1995.
- [28] J. Krause, M. Stark, J. Deng, and L. Fei-Fei. 3d object representations for fine-grained categorization. In *International IEEE Workshop on 3D Representation and Recognition (3dRR)*, 2013.
- [29] A. Krizhevsky and G. Hinton. Learning multiple layers of features from tiny images. Technical report, Citeseer, 2009.
- [30] A. Krizhevsky, I. Sutskever, and G. E. Hinton. ImageNet classification with deep convolutional neural networks. In *The Conference on Neural Information Processing Systems (NeurIPS)*, pages 1097–1105, 2012.
- [31] L. Li, K. Jamieson, G. DeSalvo, A. Rostamizadeh, and A. Talwalkar. Hyperband: A novel bandit-based approach to hyperparameter optimization. *The Journal of Machine Learning Research (JMLR)*, 18(1):6765–6816, 2017.
- [32] H. Liu, K. Simonyan, and Y. Yang. Darts: Differentiable architecture search. In *International Conference on Learning Representations (ICLR)*, 2019.
- [33] J. Lorraine, P. Vicol, and D. Duvenaud. Optimizing millions of hyperparameters by implicit differentiation. In *International Conference on Artificial Intelligence and Statistics (AISTATS)*, 2020.
- [34] I. Loshchilov and F. Hutter. SGDR: Stochastic gradient descent with warm restarts. In *International Conference on Learning Representations (ICLR)*, 2017.
- [35] D. Maclaurin, D. Duvenaud, and R. Adams. Gradient-based hyperparameter optimization through reversible learning. In *The International Conference on Machine Learning (ICML)*, pages 2113–2122, 2015.
- [36] C. J. Maddison, A. Mnih, and Y. W. Teh. The concrete distribution: A continuous relaxation of discrete random variables. In *International Conference on Learning Representations (ICLR)*, 2017.
- [37] F. Pedregosa. Hyperparameter optimization with approximate gradient. In *The International Conference on Machine Learning (ICML)*, pages 737–746, 2016.
- [38] H. Pham, M. Y. Guan, B. Zoph, Q. V. Le, and J. Dean. Efficient neural architecture search via parameter sharing. In *The International Conference on Machine Learning (ICML)*, pages 4092–4101, 2018.
- [39] P. Rajpurkar, J. Zhang, K. Lopyrev, and P. Liang. Squad: 100,000+ questions for machine comprehension of text. In *The Conference on Empirical Methods in Natural Language Processing (EMNLP)*, pages 2383–2392, 2016.
- [40] E. Real, A. Aggarwal, Y. Huang, and Q. V. Le. Regularized evolution for image classifier architecture search. In *AAAI Conference on Artificial Intelligence (AAAI)*, pages 4780–4789, 2019.
- [41] M. Sandler, A. Howard, M. Zhu, A. Zhmoginov, and L.-C. Chen. MobileNetV2: Inverted residuals and linear bottlenecks. In *Proceedings of the IEEE Conference on Computer Vision and Pattern Recognition (CVPR)*, pages 4510–4520, 2018.
- [42] A. Shaban, C.-A. Cheng, N. Hatch, and B. Boots. Truncated back-propagation for bilevel optimization. In *International Conference on Artificial Intelligence and Statistics (AISTATS)*, pages 1723–1732, 2019.

- [43] B. Shahriari, K. Swersky, Z. Wang, R. P. Adams, and N. De Freitas. Taking the human out of the loop: A review of bayesian optimization. *Proceedings of the IEEE*, 104(1):148–175, 2015.
- [44] J. Snoek, O. Rippel, K. Swersky, R. Kiros, N. Satish, N. Sundaram, M. Patwary, M. Prabhat, and R. Adams. Scalable bayesian optimization using deep neural networks. In *The International Conference on Machine Learning (ICML)*, pages 2171–2180, 2015.
- [45] C. Szegedy, W. Liu, Y. Jia, P. Sermanet, S. Reed, D. Anguelov, D. Erhan, V. Vanhoucke, and A. Rabinovich. Going deeper with convolutions. In *Proceedings of the IEEE Conference on Computer Vision and Pattern Recognition (CVPR)*, pages 1–9, 2015.
- [46] M. Tan, B. Chen, R. Pang, V. Vasudevan, M. Sandler, A. Howard, and Q. V. Le. MNasNet: Platform-aware neural architecture search for mobile. In *Proceedings of the IEEE Conference on Computer Vision and Pattern Recognition (CVPR)*, pages 2820–2828, 2019.
- [47] M. Tan and Q. Le. EfficientNet: Rethinking model scaling for convolutional neural networks. In *The International Conference on Machine Learning (ICML)*, pages 6105–6114, 2019.
- [48] M. Tan, R. Pang, and Q. V. Le. EfficientDet: Scalable and efficient object detection. In *Proceedings of the IEEE Conference on Computer Vision and Pattern Recognition (CVPR)*, 2020.
- [49] C. Thornton, F. Hutter, H. H. Hoos, and K. Leyton-Brown. Auto-weka: Combined selection and hyperparameter optimization of classification algorithms. In *The SIGKDD International Conference on Knowledge Discovery and Data Mining*, pages 847–855, 2013.
- [50] B. Wu, X. Dai, P. Zhang, Y. Wang, F. Sun, Y. Wu, Y. Tian, P. Vajda, Y. Jia, and K. Keutzer. FBNet: Hardware-aware efficient convnet design via differentiable neural architecture search. In *Proceedings of the IEEE Conference on Computer Vision and Pattern Recognition (CVPR)*, pages 10734–10742, 2019.
- [51] L. Xie and A. Yuille. Genetic CNN. In *Proceedings of the IEEE International Conference on Computer Vision (ICCV)*, pages 1379–1388, 2017.
- [52] S. Xie, H. Zheng, C. Liu, and L. Lin. SNAS: stochastic neural architecture search. In *International Conference on Learning Representations (ICLR)*, 2019.
- [53] C. Ying, A. Klein, E. Christiansen, E. Real, K. Murphy, and F. Hutter. Nas-bench-101: Towards reproducible neural architecture search. In *The International Conference on Machine Learning (ICML)*, pages 7105–7114, 2019.
- [54] A. Zela, A. Klein, S. Falkner, and F. Hutter. Towards automated deep learning: Efficient joint neural architecture and hyperparameter search. In *The International Conference on Machine Learning (ICML Workshop)*, 2018.
- [55] B. Zoph and Q. V. Le. Neural architecture search with reinforcement learning. In *International Conference on Learning Representations (ICLR)*, 2017.
- [56] B. Zoph, V. Vasudevan, J. Shlens, and Q. V. Le. Learning transferable architectures for scalable image recognition. In *Proceedings of the IEEE Conference on Computer Vision and Pattern Recognition (CVPR)*, pages 8697–8710, 2018.